Unexpected nascent atmospheric emissions of three ozone-depleting hydrochlorofluorocarbons

Martin K. Vollmer[a,1], Jens Mühle[b], Stephan Henne[a], Dickon Young[c], Matthew Rigby[c], Blagoj Mitrevski[d], Sunyoung Park[e], Chris R. Lunder[f], Tae Siek Rhee[g], Christina M. Harth[b], Matthias Hill[a], Ray L. Langenfelds[d], Myriam Guillevic[a], Paul M. Schlauri[a], Ove Hermansen[f], Jgor Arduini[h,i], Ray H. J. Wang[j], Peter K. Salameh[b], Michela Maione[h,i], Paul B. Krummel[d], Stefan Reimann[a], Simon O'Doherty[c], Peter G. Simmonds[c], Paul J. Fraser[d], Ronald G. Prinn[k], Ray F. Weiss[b], and L. Paul Steele[d]

[a]Laboratory for Air Pollution and Environmental Technology, Empa, Swiss Federal Laboratories for Materials Science and Technology, 8600 Dübendorf, Switzerland; [b]Scripps Institution of Oceanography, University of California San Diego, La Jolla, CA 92093; [c]Atmospheric Chemistry Research Group, School of Chemistry, University of Bristol, Bristol BS8 1TL, United Kingdom; [d]Climate Science Centre, CSIRO Oceans and Atmosphere, Commonwealth Scientific and Industrial Research Organisation, Aspendale, VIC 3195, Australia; [e]Department of Oceanography, Kyungpook National University, Daegu 41566, South Korea; [f]Monitoring and Instrumentation Technology Department, Norwegian Institute for Air Research, 2007 Kjeller, Norway; [g]Division of Ocean Sciences, Korea Polar Research Institute, Incheon 21990, South Korea; [h]Department of Pure and Applied Sciences, University of Urbino, 61029 Urbino, Italy; [i]Institute of Atmospheric Sciences and Climate, Italian National Research Council, 40129 Bologna, Italy; [j]School of Earth and Atmospheric Sciences, Georgia Institute of Technology, Atlanta, GA 30332; and [k]Center for Global Change Science, Massachusetts Institute of Technology, Cambridge, MA 02139

Edited by Susan Solomon, Massachusetts Institute of Technology, Cambridge, MA, and approved December 7, 2020 (received for review May 28, 2020)

Global and regional atmospheric measurements and modeling can play key roles in discovering and quantifying unexpected nascent emissions of environmentally important substances. We focus here on three hydrochlorofluorocarbons (HCFCs) that are restricted by the Montreal Protocol because of their roles in stratospheric ozone depletion. Based on measurements of archived air samples and on in situ measurements at stations of the Advanced Global Atmospheric Gases Experiment (AGAGE) network, we report global abundances, trends, and regional enhancements for HCFC-132b ($CH_2ClCClF_2$), which is newly discovered in the atmosphere, and updated results for HCFC-133a (CH_2ClCF_3) and HCFC-31 (CH_2ClF). No purposeful end-use is known for any of these compounds. We find that HCFC-132b appeared in the atmosphere 20 y ago and that its global emissions increased to 1.1 Gg·y^{-1} by 2019. Regional top-down emission estimates for East Asia, based on high-frequency measurements for 2016–2019, account for ∼95% of the global HCFC-132b emissions and for ∼80% of the global HCFC-133a emissions of 2.3 Gg·y^{-1} during this period. Global emissions of HCFC-31 for the same period are 0.71 Gg·y^{-1}. Small European emissions of HCFC-132b and HCFC-133a, found in southeastern France, ceased in early 2017 when a fluorocarbon production facility in that area closed. Although unreported emissive end-uses cannot be ruled out, all three compounds are most likely emitted as intermediate by-products in chemical production pathways. Identification of harmful emissions to the atmosphere at an early stage can guide the effective development of global and regional environmental policy.

Montreal Protocol | atmospheric composition | ozone depletion

Localizing and quantifying halocarbon emissions from atmospheric observations and transport modeling has become an important tool to validate emissions derived from activity data and emission factors (1–7). This can also be used to detect new substances and derive their nascent trends and emissions, thereby playing an important role as an early warning system leading to improved environmental emissions policies.

Here, we present long-term emissions of three ozone-depleting substances (ODSs) which have no reported end-use. The emissive use of these substances is regulated by the Montreal Protocol on Substances that Deplete the Ozone Layer and its Amendments (hereafter referred to as the Montreal Protocol). The Montreal Protocol is an international agreement that regulates the phase-out of production and consumption of ODSs. The environmental target of these regulations is to lower ODS abundances in the atmosphere to safeguard the stratospheric ozone layer. The full ban on production and consumption for emissive end-use of the primary ODSs, the chlorofluorocarbons (CFCs), was set to the mid-1990s for developed (non-Article 5) countries and to 2010 globally. As a consequence, emissions have been declining when calculated based on production and consumption (bottom-up). Unexpectedly, though, emissions inferred from atmospheric observations (top-down method) of several ODSs were recently found to be declining more slowly than expected, or even increasing (4, 5, 8–10). This raised concerns about potential violations of the Montreal Protocol (4, 5, 11). However, it is difficult to prove a violation, because emissions are aggregated when using the top-down method, and additionally include those from banked ODSs in end-user products (e.g., refrigerators or foams), which are not controlled by the Montreal Protocol (12). Further, emissions from feedstock and process agents, and from inadvertent or coincidental production during

Significance

We demonstrate the need to detect and track unexpected substances in the atmosphere and to locate their sources. Here, we report on three hydrochlorofluorocarbons (HCFCs) that have no known end-uses. HCFC-132b ($CH_2ClCClF_2$) is newly discovered in the global atmosphere. We identify East Asia as the dominant source region for global emissions of this compound and of HCFC-133a (CH_2ClCF_3). We also quantify global emissions of HCFC-31 (CH_2ClF). These compounds are most likely emitted as intermediate by-products of chemical production processes. The early discovery and identification of such unexpected emissions can identify the related industrial practices and help to develop and manage environmental policies to reduce unwanted and potentially harmful emissions before the scale of the problem becomes more costly to mitigate.

Author contributions: M.K.V., J.M., B.M., S.P., M.M., P.B.K., S.R., S.O., P.G.S., P.J.F., R.G.P., R.F.W., and L.P.S. designed the experiment; M.K.V., J.M., D.Y., B.M., C.R.L., T.S.R., C.M.H., M.H., R.L.L., M.G., P.M.S., O.H., J.A., S.O., and L.P.S. provided samples, calibrations, and/or made the measurements; S.H. and M.R. made the model calculations; P.K.S. wrote software; R.H.J.W. and P.K.S. processed data; and M.K.V. wrote the paper with contributions from all coauthors.

The authors declare no competing interest.

This article is a PNAS Direct Submission.

[1]To whom correspondence may be addressed. Email: Martin.Vollmer@empa.ch.

This article contains supporting information online at https://www.pnas.org/lookup/suppl/doi:10.1073/pnas.2010914118/-/DCSupplemental.

Published January 25, 2021.

a manufacturing process, are also included in these aggregated top-down emission estimates. Although the Montreal Protocol addresses this group of emissions, no stringent control is enforced to date, with the parties primarily being urged to take steps to minimize such emissions (11, 13, 14). Attention has so far been limited to only a small number of compounds, notably carbon tetrachloride (CCl_4), whose emissions are not declining as expected, partially due to unreported nonfeedstock emissions (3, 15).

The three ODSs identified in this study are all hydrochlorofluorocarbons (HCFCs), which have lower potentials than CFCs to harm the ozone layer, and which have been used in the past as interim replacements for CFCs. Their phase-out by the Montreal Protocol was significantly tightened in 2007, with a complete ban in 2020 for developed (non-Article 5) countries and 2030 globally. HCFCs have also been included in the baseline calculations under the Kigali Amendment in 2016 to facilitate "leap-frogging" high global warming potential (GWP) hydrofluorocarbons (HFCs) by directly replacing HCFCs with low-GWP substances (16, 17). Similar to the CFCs, the major HCFCs, HCFC-22 ($CHClF_2$), HCFC-142b (CH_3CClF_2), and HCFC-141b (CH_3CCl_2F), are used in stationary refrigeration and structural foam blowing. Their global emissions have leveled or started to decline over the past years as a consequence of their production phase-down (18).

We report on the newly detected HCFC-132b (1,2-dichloro-1,1-difluoroethane; $CH_2ClCClF_2$) in the atmosphere and present substantial updates on abundance and emissions for the previously found HCFC-133a and HCFC-31 (8, 19, 20). Their lack of known end-uses gives rise to speculation about their sources and their roles within the framework of the Montreal Protocol. There are no public inventories or bottom-up emission reports available for these compounds. Although their physical and chemical properties are suitable for applications in refrigeration and other industrial applications, their toxicities and carcinogenicities have prevented consumer end-use applications in the past (21–25). Their removal from the atmosphere is mainly driven by reaction with the hydroxyl radical (OH), leading to global atmospheric lifetimes of 3.5 y for HCFC-132b, 4.6 y for HCFC-133a, and 1.2 y for HCFC-31 (26).

The measurements presented here have wide geographical and temporal coverage, based on ongoing in situ ground-based measurements at the stations of the Advanced Global Atmospheric Gases Experiment (AGAGE) network (27). Our records also include measurements of archived air samples from the Southern Hemisphere (SH) Cape Grim Air Archive (CGAA) starting in 1978 and from the Northern Hemisphere (NH), as well as multiyear weekly collected air samples from Antarctica. We also extend the previous record of HCFC-133a with in situ AGAGE and new CGAA measurements (8, 19). Furthermore, we present a longer record for HCFC-31 than was previously available (20), through measurements of the CGAA, and updated contemporary observations from Antarctic samples (2015–2019) and NH measurements from Dübendorf (Switzerland).

Using these measurements, an inverse method, and the AGAGE 12-box atmospheric transport model, we estimate hemispheric emissions and reconstruct abundances of the three HCFCs from 1978 to the present (28, 29). Based on the large pollution events recorded at the AGAGE station, Gosan (Jeju Island, South Korea), we also estimate regional East Asian emissions of HCFC-132b and HCFC-133a using a regional inverse-modeling system (30).

Results

Global Atmospheric Distributions of the HCFCs. We calculated hemispheric long-term trends by combining flask measurements with in situ high-resolution observations from AGAGE stations (Fig. 1). HCFC-132b first appeared in the NH atmosphere in the late 1990s, followed by a sustained and rapid growth to a dry air mole fraction of 0.15 parts per trillion (ppt) by 2013 (Fig. 1*A*). After a short decline until 2016, the compound increased again to a maximum of 0.17 ppt by the end of 2019. The SH abundances lagged the NH abundances and remained lower throughout the entire record, indicating that emissions of this compound predominantly occurred in the NH. The absence of HCFC-132b from the atmosphere before 1995 (*SI Appendix*) suggests an entirely anthropogenic origin.

HCFC-133a exhibits a general increase in both hemispheres. Measurements of archived air from the US West Coast detail a pronounced reversal in the NH abundance in 2007/2008, in agreement with a similar feature found for the SH (8). Also, independent measurements of the CGAA confirm earlier findings, in particular, the presence of this compound in the SH atmosphere before 1978 (8). New flask and in situ measurements for 2015–2019 reveal that the downward trend of HCFC-133a in the NH (2012–2015; ref. 19) has reversed, and the compound has increased to >0.5 ppt again.

For HCFC-31, first detectable mole fractions appeared in samples from the late 1990s. Following more than a decade-long growth, we find, similar to HCFC-133a, a decline of HCFC-31 in

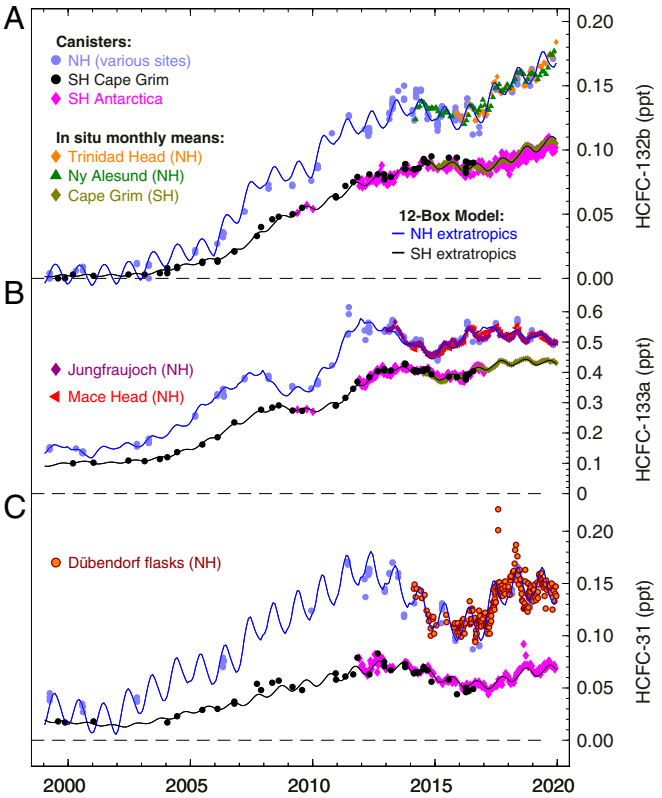

Fig. 1. Atmospheric observations and model reconstructions of the HCFCs, HCFC-132b (*A*), HCFC-133a (*B*), and HCFC-31 (*C*). Units are dry air mole fractions in ppt (pmol·mol^{-1}). The ∼40-y-long records are limited here to 1999–2019 for better temporal resolution. Flask-sample results from various NH sites are aggregated into a single dataset for clarity. Flask samples for the SH are shown for Cape Grim (CGAA, Tasmania) and the Antarctic station King Sejong. In situ records for HCFC-132b and HCFC-133a from stations of the AGAGE are shown here as background-filtered monthly means for a few illustrative stations only. Modeled records, derived from the observations and an inversion system using a 12-box chemical transport model, are shown for the four ground-level model boxes.

the atmosphere for 2012–2015, which was followed by another strong increase and a stabilization over the past 3 y.

There are surprising similarities in the records of the three compounds (Fig. 1). Compared to known records for many other halocarbons, we find large multiyear variability in these records, pointing to rapidly changing emissions. The most pronounced feature is a temporal maximum in abundances for all three compounds within the period 2012–2014, although not exactly synchronous.

Global Emissions. Global emissions for all three compounds show a generally increasing trend over the last two decades, with mean values for 2016–2019 of 0.97 Gg·y^{-1} for HCFC-132b, 2.3 Gg·y^{-1} for HCFC-133a, and 0.71 Gg·y^{-1} for HCFC-31 (Fig. 2). However, we calculated a large relative variability in these emissions, particularly for HCFC-133a. This variability is unusual compared to other widely used synthetic halocarbons (18) and indicates that a major fraction of these emissions does not originate from banks (compounds stored in equipment, which are usually emitted slowly over time and, hence, only exhibit small variability in their global emissions). It further suggests that the emissions are not deriving from impurities in commercially used halocarbons, which generally show temporally much smoother emission trends. Note that the emissions uncertainties in Fig. 2 are dominated by uncertainties in the lifetime, which act like potential biases across all years. Therefore, in our global inversions, the year-to-year variability is better constrained than the absolute emissions magnitude, particularly for HCFC-132b, which has a relatively large lifetime uncertainty.

Twenty-year cumulative emissions (1978–2019) for HCFC-132b, HCFC-133a, and HCFC-31 amount to 13 Gg, 44 Gg, and 10.6 Gg, respectively. Given their relatively small ozone-depletion potentials (ODPs), compared to the primary ODSs, of 0.038, 0.019, and 0.019, respectively, (26), we calculated a combined cumulative emission of 1.5 Gg-ODP-weighted. Although their impacts on stratospheric ozone degradation are small and roughly one order of magnitude smaller compared to the recently found yearly unexpected emissions of CFC-11 (CCl_3F) (4, 5), their absolute emissions are significant, particularly for compounds with no purposeful end-use.

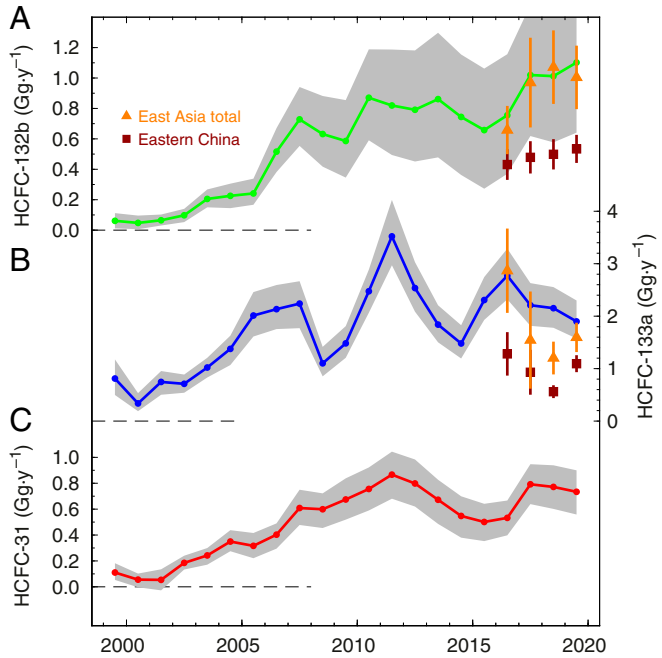

Fig. 2. Global and East Asia regional emissions of the HCFCs HCFC-132b (*A*), HCFC-133a (*B*), and HCFC-31 (*C*). Shaded gray bands denote the 16/84-percentile uncertainty range for the global emissions. Total emissions from East Asia (orange) and Eastern China only (maroon) are plotted for HCFC-132b and HCFC-133a with 95% confidence intervals (gray shading).

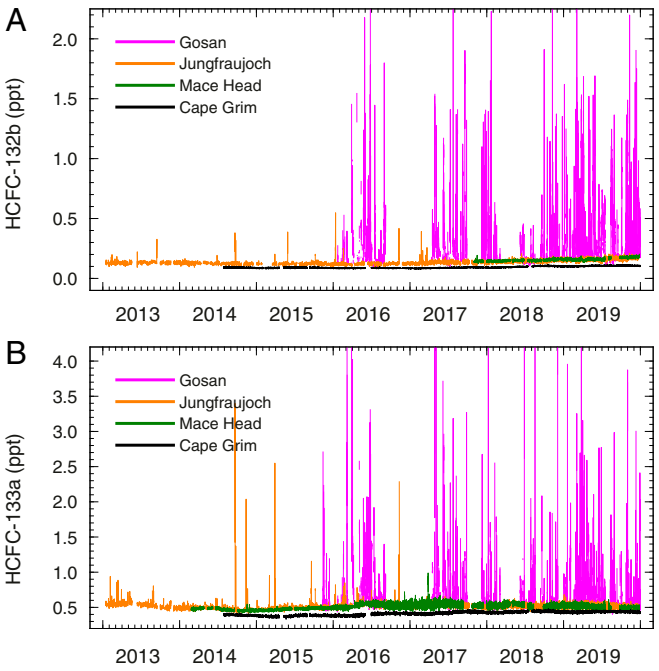

Fig. 3. High-resolution measurement records of HCFC-132b (*A*) and HCFC-133a (*B*) from selected stations of the AGAGE. Pollution events recorded at the Gosan station (South Korea), where measurements started in 2015/2016, strongly exceed those at all other stations in frequency and magnitude.

Emissions from East Asia. Within the AGAGE network, frequent and large (up to 4 ppt) pollution events for HCFC-132b and HCFC-133a were recorded at the South Korean station, Gosan, indicating substantial regional emissions (Fig. 3; HCFC-31 is not measured at the AGAGE sites; *Measurement Methods*). By combining these records with an inverse-modeling method (30), we find that the most concentrated emissions in East Asia (defined as China, Taiwan, North and South Korea, and Japan) occur in Eastern China (Figs. 2 and 4). For HCFC-132b, Eastern China emissions are 0.43 to 0.53 Gg·y^{-1} for 2016–2019 and account, on average, for 50% of global emissions (Fig. 2*A*). The East Asia total emissions account for ∼95% of the global emissions, within the uncertainties of the methods. The inversion also attributes a large fraction of East Asian emissions to West China. However, due to the reduced sensitivity of the observational site to West China, these estimates are connected with a much larger uncertainty than for East China. For HCFC-133a, Eastern China emissions account, on average, for 43% of the global emissions, and East Asia emissions explain ∼80% of the global emissions (Fig. 2*B*).

There is a distinct difference in the geographical distribution of the emissions from Eastern China (Fig. 4). For HCFC-132b, the strongest source region is found in northeastern China (Shangdong and Southern Hebei). In contrast, for HCFC-133a, the highest emissions are found in the Shanghai region. Both regions were recently identified as strong emitters of other halocarbons, but the predominance of HCFC-132b and HCFC-133a emissions to only one of these two regions is unusual (10, 31).

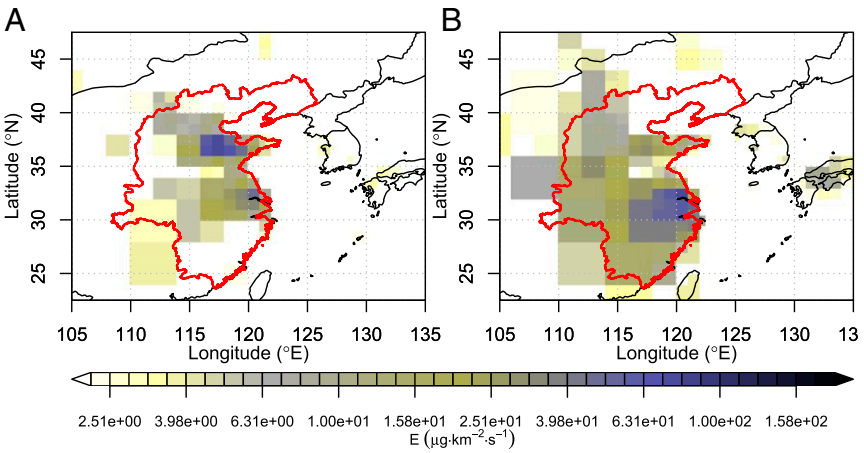

Fig. 4. Posterior HCFC-132b (*A*) and HCFC-133a (*B*) emission distributions ($\mu g \cdot km^{-2} \cdot s^{-1}$) for eastern China based on observations at Gosan (Jeju Island, South Korea) for 2016–2019. The red line encloses the area defined as East China.

Both areas host intense fluorocarbon industry, which could support speculations on feedstock/by-product emissions. For CCl_4, another ODS with little-known allowed emissive end-uses, a study covering 2009–2016 found that emissions first originated in the Shanghai region, but then spread out to include northern Chinese provinces (32). Recent similar high-emission regions were also found for CFC-11 with suggested ultimate emissive end-use (5).

Sources in Western Europe. We find much smaller and highly sporadic (two to three times per year) pollution events for HCFC-132b (up to 0.5 ppt) and HCFC-133a (up to 3.5 ppt) at some of the European stations (mainly Jungfraujoch and Monte Cimone). Surprisingly, European pollution events for HCFC-132b ceased by early 2017, and those for HCFC-133a became even less frequent (*SI Appendix*), indicating that regional emissions were greatly reduced. For the period before April 2017, our analysis reveals strong emissions of HCFC-133a near Lyon in southeastern France, similar to those found earlier using a reduced dataset (19), and weaker HCFC-132b emissions close by. The emissions in this region of intense fluorochemical production ceased after April 2017, and only a secondary potential source of HCFC-133a remains in western Germany. The cessation of measured HCFC-132b and HCFC-133a pollution events in early 2017 could indicate a change in the manufacturing processes in relevant production plants in the area. A possible explanation is the cessation of HFC-134a (CH_2FCF_3) production at Pierre-Bénite (Lyon) in the first quarter of 2017 (33).

Discussion

HCFC-133a and HCFC-31 in the global atmosphere were previously assumed to originate from factory-level emissions during the production of mainly HFC-134a and HFC-143a (CH_3CF_3) and HFC-32 ($CHCl_2F$), respectively (8, 14, 20, 34, 35). HCFC-132b is also likely an intermediate/by-product involved in reactions to produce HFC-134a and perhaps other HFCs, though we cannot exclude end-use applications. For example, in the widely used reaction of trichloroethylene ($CHCl{=}CCl_2$) with hydrogen fluoride (HF) to produce HFCs (foremost HFC-134a), the intermediates $CH_2Cl\text{-}CFCl_2$ (HCFC-131a), $CH_2Cl\text{-}CClF_2$ (HCFC-132b), and $CH_2Cl\text{-}CF_3$ (HCFC-133a) could potentially be produced and leak to the atmosphere (36). The other isomers of dichlorodifluoroethane are not likely produced from hydrofluorination of HCFC-131a, as this would require hydrogen (H) rearrangement, in the case of CHClF-CHClF (HCFC-132) and $CHCl_2\text{-}CHF_2$ (HCFC-132a), or nucleophilic substitution of chlorine (Cl) by fluorine (F) on the less favorable carbon atom in the case of $CH_2F\text{-}CCl_2F$ (HCFC-132c). This may explain why we did not find these three compounds in the global atmosphere.

Our finding of a strong source of HCFC-133a (and, to a lesser extent, also of HCFC-132b) in France potentially supports this hypothesis, in particular, given the lack of recorded pollution events for both compounds, starting with the cessation of the HFC-134a production in that region. On the other hand, for the other (and only remaining) European HFC-134a production site near Frankfurt, HCFC-133a emissions are detected with our method, while those for HCFC-132b are arguably undetectable (Fig. 5 and *SI Appendix*).

For the globally dominant emissions, which we locate in East Asia, the predominant source regions for HCFC-132b and HCFC-133a are located in different places. Assuming that both substances are emitted mainly during HFC-134a production, this separation and the large temporal global emission variability, despite monotonically increasing global HFC-134a production, suggest that the generation and leaks of HCFC-132b and HCFC-133a (and HCFC-31 in the case of HFC-32 production) are highly sensitive to industrial practices at the individual HFC production facilities.

Conclusions and Significance

In addition to targeting ODS end-use applications, the Montreal Protocol also addresses feedstock and process emissions, however, with currently no stringent control. The need to place adequate emphasis on these emissions is demonstrated by the example of CCl_4, a compound for which large global unaccounted emissions are found, a large fraction of which are unreported and believed to derive from current industrial production processes (3, 15). We report on emissions of three other ODSs which most likely fall into this category. Our findings of geographical source separations and large temporal variabilities in the global emissions suggest that some factories temporarily emit much more process-intermediate HCFCs than the low percentages of the end-use compound (HFC) that are commonly assumed (14). These should be identified, and measures applied for emission reductions, according to the recommendations of the Montreal Protocol.

While the emissions of these three HCFCs are quantifiable and have increased over the last decades, their ODP-weighted impacts are small compared to those of the major ODSs. Nevertheless, our findings demonstrate a method for early warning

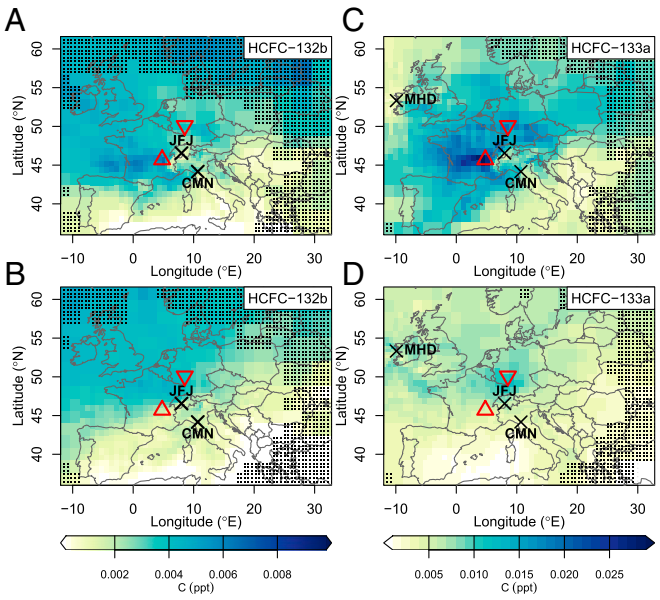

Fig. 5. Potential source areas for European emissions of HCFC-132b and HCFC-133a, as estimated by footprint statistics (*SI Appendix*). Units refer to average mole fraction enhancements at the receptor sites when influenced by a given grid cell. *A* and *C* are for 2014–March 2017, and *B* and *D* are for April 2017–2019. This temporal distinction is made based on the lack of significant pollution events after March 2017. Stations are Mace Head (MHD; Ireland), Jungfraujoch (JFJ; Switzerland), and Monte Cimone (CMN ; Italy). Triangles denote HFC-134a factories in France (upward triangle) and Germany (downward triangle). Dotted areas have low source sensitivities and should not be interpreted.

detection and quantification of nascent emissions of synthetic trace gases based on atmospheric observations. This can, in turn, help to validate inventory-based emissions estimates, uncover potential unreported sources, and enable the assessment of the effectiveness of subsequent mitigation efforts. From an economic perspective, early discovery also enables processes to be changed to reduce unwanted emissions before the scale of the problem becomes more costly to mitigate, as has unfortunately been the case for unaccounted emissions of other compounds (1–7).

More broadly, this study demonstrates the analytical power of modern atmospheric monitoring instrumentation to detect atmospheric abundances at sub-ppt level arising from nascent industrial emissions. It also demonstrates the importance of large-scale global atmospheric network observations and modeling for identifying and quantifying regional emissions. As industrialization continues to expand and move into new regions, the absence of broader regional coverage for such atmospheric observations inhibits a full reconciliation between emissions measured in the global atmosphere and the sum of those determined regionally. The expansion of observational networks will be needed to close such gaps in support of the protection of the stratospheric ozone layer and the climate.

Materials and Methods

Site Description. The AGAGE global network consists of nine fully intercalibrated field stations with long-term measurement records of a suite of ODSs (27). The network is complemented by affiliated stations and by laboratory instruments, which also serve as urban stations. European field stations are Zeppelin (Spitsbergen), Mace Head (Ireland), Jungfraujoch (Swiss Alps), and the affiliated station Monte Cimone (Italy). Asian stations are located at Gosan (Jeju Island, South Korea) and Shangdianzi (China); however, data from the latter could not be used for this study. Other stations are Trinidad Head (California), Ragged Point (Barbados), Cape Matatula (American Samoa), and Cape Grim (Tasmania, Australia). Measurement records for HCFC-132b and HCFC-133a are of various lengths, with the longest at Jungfraujoch, starting in 2013. In addition to the in situ measurements, flask samples contribute to the analysis presented here. Canister samples are collected weekly at the South Korean Antarctic Station King Sejong (King George Island, South Shetland Islands) (37). Archived air samples used in our analysis derive from the CGAA, which is a set of >120 samples collected since 1978 at the Cape Grim Baseline Air Pollution Station (38–41). Additional archived air samples were collected under clean-air conditions in the NH, mostly at Trinidad Head, La Jolla (California), Boulder (Colorado), and in the Swiss Alps (42).

Measurement Methods. All measurements presented here were conducted using "Medusa" preconcentration gas chromatography mass spectrometry (GC-MS) instrumentation used in AGAGE (27, 43, 44). HCFC-132b was identified along with the other three isomers of dichlorodifluoroethane to conclusively demonstrate the absence of interferences. Also, with first weekly atmospheric measurements of these three additional isomers, starting in mid-2019, and detection levels of ∼0.005 ppt, we find these compounds undetectable within the airmass footprint of the urban station Dübendorf (Switzerland). Due to their atmospheric lifetimes >1 y (17), we conclude that these three isomers are currently also undetectable in the global atmosphere.

Analytical details for HCFC-133a and HCFC-31 are given in earlier studies (19, 20). Since then, HCFC-133a measurements have been fully integrated into the AGAGE network, from which global high-resolution data are now available. Analysis of HCFC-31 is hampered by a coelution with CFC-12 on aged Porabond Q columns (used in AGAGE) and has therefore not been integrated into the network. The HCFC-31 flask-sample measurements used in this study were made on the Empa laboratory Medusa-GC-MS in a batch mode using a column on which the two compounds could be fully separated and on a GasPro column on the Commonwealth Scientific and Industrial Research Organization (CSIRO) laboratory Medusa (Medusa-9) for the CGAA samples.

Calibration. The present work prompted the development of the Swiss Federal Office of Metrology (METAS) METAS-2017 primary calibration scale for HCFC-132b (45). It is based on 11 dynamically gravimetrically prepared, Système International-traceable primary reference standards ranging from 0.9 to 1.5 ppt. The calibration scale was adopted into the AGAGE-based Scripps Institution of Oceanography (SIO) R1 calibration-measurement database and allowed for a reporting of fully intercalibrated measurements used here. The estimated accuracy of this calibration scale is 1.6% (2σ). Measurements of HCFC-133a are also fully intercalibrated and are based on the Empa-2013 primary calibration scale with an estimated accuracy of 10% (2σ) (19). For HCFC-132b and HCFC-133a, the calibration scales were propagated from the SIO pool of secondary standards through tertiary traveling standards to on-site quaternary (working) standard. For HCFC-31, the Empa and CSIRO laboratory measurements were intercalibrated, and results are based on the Empa-2013 primary calibration scale (20).

Global Emissions Derived from Global Chemical Transport Model and Inverse Methods. To derive global emissions that are based on baseline atmospheric observations ("top-down"), we employed the AGAGE 12-box model (46–50). The model divides the atmosphere into four zonal bands, separated at the Equator and at the 30° latitudes, thereby creating boxes of similar air masses. The vertical box separations are at 500 and 200 hPa. We included temperature-dependent hydroxyl (OH) radical reactions, which are the main removal mechanism of all three compounds from the atmosphere (51). We assumed stratospheric lifetimes of 45 y for HCFC-132b, 103 y for HCFC-133a, and 35 y for HCFC-31 (26), leading to overall atmospheric lifetimes of 3.4 y for HCFC-132b, 4.5 y for HCFC-133a, and 1.4 y for HCFC-31 in the box model.

Emissions were inferred by comparing model simulations to baseline observations using a Bayesian inverse method in which the emissions growth rate was weakly constrained a priori (29). High-frequency observations were filtered to remove "pollution events" using a statistical filter (28) and, combined with archived air samples, averaged into semihemispheres. The uncertainty on the observations combined two terms, one related to the measurement repeatability and one related to the ability of the model to represent the data. The latter was assumed to be equal to the baseline variability for high-frequency samples (or, for flask samples, the average high-frequency variability in the same hemisphere, scaled by mole fraction difference between the flask and high-frequency observations). Some seasonality in emissions was imposed by fitting a sine curve to the

emissions, which minimized the model–data mismatch (19). Given the lack of available prior emissions estimates, the annual emissions growth rate was assumed to be zero a priori, with an uncertainty assumed to be 0.1, 1, and 0.1 $Gg \cdot y^{-2}$ for HCFC-132b, HCFC-133a, and HCFC-31, respectively. The derived emissions were found to not strongly depend on these values. The uncertainties in the a posteriori emissions estimates combined uncertainties related to the measurements, model representation error, prior constraint, atmospheric lifetime, and calibration-scale uncertainty (29). The uncertainty in the lifetime was assumed to be 20% for HCFC-31 (20). For HCFC-133a and HCFC-132b, we assumed lifetime uncertainties equal to the uncertainty in the rate constant with respect to reaction with the hydroxyl radical [10% for HCFC-133a and 50% for HCFC-132b (51)], which we assumed to be the largest term in the lifetime uncertainty budget for these substances.

Regional Emission Estimates. The inversion system used to estimate East Asian regional emissions has been documented (5, 30). It is here applied to HCFC-132b and HCFC-133a for 2016–2019 and using observations from Gosan alone, for which pollution events were identified and quantified by subtracting a smooth statistical baseline fit from the observations (52). Source sensitivities were computed with the Lagrangian particle-dispersion model FLEXPART (version 9.2-Empa) driven by operational analysis and forecasts from the European Center for Medium-Range Weather Forecasts Integrated Forecasting System employing a horizontal resolution of $0.2^\circ \times 0.2^\circ$ in the area of interest. The Bayesian inversion for East Asia was carried out by using a flat a priori emission distribution over all land areas, reflecting our expectation that the emissions are not end-user-related and, hence, don't follow population densities. A priori and data-mismatch covariance matrices were constructed by using a maximum-likelihood approach (30). For European HCFC emissions, the inversion system showed very little skill in reproducing the observed peak concentrations and was consistent with emissions originating from intermittent sources. Therefore, we applied a more qualitative method to identify potential source areas, which can be seen as a spatially distributed, weighted averaging of the observed concentration increments and builds on a method termed "trajectory statistics" (53) (*SI Appendix*).

Data Availability. In situ measurements of HCFC-132b and HCFC-133a from the AGAGE stations are available through the AGAGE website (https://agage.mit.edu/). Measurements of the samples collected in flasks, such as for archived air, Antarctica and Dübendorf (HCFC-31), and model results, are accessible through https://zenodo.org (DOI: 10.5281/zenodo.4266485).

ACKNOWLEDGMENTS. We acknowledge the station personnel at all stations for their continuous support in conducting in situ measurement. Support is also acknowledged for canister sampling at Cape Grim (CSIRO and Bureau of Meteorology), King Sejong (KOPRI), SIO, and for the Dübendorf HCFC-31 record (numerous helpers). We thank Archie McCulloch for valuable discussions on the industrial synthesis of HFC-134a and possible by-products. The joint CGAA project is operated by CSIRO and the Australian Bureau of Meteorology. AGAGE operations at Mace Head, Trinidad Head, Cape Matatula, Ragged Point, and Cape Grim are supported by NASA Grants NAG5-12669, NNX07AE89G, NNX11AF17G, and NNX16AC98G (to MIT) and NNX07AE87G, NNX07AF09G, NNX11AF15G, and NNX11AF16G (to SIO); Department for Business, Energy & Industrial Strategy (BEIS) Contract 1028/06/2015 (to the University of Bristol for Mace Head and Tacolneston); National Oceanic and Atmospheric Administration (NOAA) Contracts RA-133-R15-CN-0008 and 1305M319CNRMJ0028 (to the University of Bristol for Barbados, by CSIRO Australia); the Bureau of Meteorology (Australia); the Department of Environment and Energy (Australia); and Refrigerant Reclaim Australia. Financial support for the measurements at the other stations was provided as follows: for Jungfraujoch, by the Swiss National Programs HALCLIM and CLIMGAS-CH (Swiss Federal Office for the Environment [FOEN]) and by the International Foundation High Altitude Research Stations Jungfraujoch and Gornergrat (HFSJG); for Zeppelin, by the Norwegian Environment Agency; for Monte Cimone, by the National Research Council of Italy and the Italian Ministry of Education, University and Research through the Project of National Interest Nextdata; and for Gosan, by the Kyungpook National University Research Fund, 2018. Support for King Sejong flask samples comes from the Swiss State Secretariat for Education and Research and Innovation (SERI); the National Research Foundation of Korea for the Korean-Swiss Science and Technology Cooperation Program; and the Korean Polar Research Programs PE13410 and PE21140. M.K.V. was supported by FOEN and 2016 grants from Empa and the Swiss National Science Foundation (SNSF) for technical development and archived air and firn air measurements at CSIRO Aspendale.

1. R. F. Weiss, R. G. Prinn, Quantifying greenhouse-gas emissions from atmospheric measurements: A critical reality check for climate legislation. *Philos. Trans. R. Soc. London, Ser. A* **369**, 1925–1942 (2011).
2. T. Arnold et al., Nitrogen trifluoride global emissions estimated from updated atmospheric measurements. *Proc. Natl. Acad. Sci. U.S.A.* **110**, 2029–2034 (2013).
3. Q. Liang, P. A. Newman, S. Reimann, "SPARC report on the mystery of carbon tetrachloride" (SPARC Tech. Rep. 7, WCRP-13/2016, ETH Zurich Institute for Atmospheric and Climate Science, Zurich, Switzerland, 2016).
4. S. A. Montzka *et al.*, An unexpected and persistent increase in global emissions of ozone-depleting CFC-11. *Nature* **557**, 413–417 (2018).
5. M. Rigby *et al.*, Increase in CFC-11 emissions from eastern China based on atmospheric observations. *Nature* **569**, 546–550 (2019).
6. P. G. Simmonds *et al.*, The increasing atmospheric burden of the greenhouse gas sulfur hexafluoride (SF_6). *Atmos. Chem. Phys.* **20**, 7271–7290 (2020).
7. K. M. Stanley *et al.*, Increase in global emissions of HFC-23 despite near-total expected reductions. *Nat. Commun.* **11**, 397 (2020).
8. J. C. Laube *et al.*, Newly detected ozone-depleting substances in the atmosphere. *Nat. Geosci.* **7**, 266–269 (2014).
9. K. E. Adcock *et al.*, Continued increase of CFC-113a (CCl_3CF_3) mixing ratios in the global atmosphere: Emissions, occurrence and potential sources. *Atmos. Chem. Phys.* **18**, 4737–4751 (2018).
10. M. K. Vollmer *et al.*, Atmospheric histories and emissions of chlorofluorocarbons CFC-13 ($CClF_3$), ∑CFC-114 ($C_2Cl_2F_4$), and CFC-115 (C_2ClF_5). *Atmos. Chem. Phys.* **18**, 979–1002 (2018).
11. S. Solomon, J. Alcamo, A. R. Ravishankara, Unfinished business after five decades of ozone-layer science and policy. *Nat. Commun.* **11**, 4272 (2020).
12. M. Lickley *et al.*, Quantifying contributions of chlorofluorocarbon banks to emissions and impacts on the ozone layer and climate. *Nat. Commun.* **11**, 1380 (2020).
13. United Nations Environment Programme, "Handbook for the Montreal Protocol on substances that deplete the ozone layer" (Tech. Rep., United Nations Environment Programme, Nairobi, Kenya, ed. 13, 2017).
14. M. Miller, T. Batchelor, "Information paper on feedstock uses of ozone-depleting substances" (European Commission Service Contract No. 07.1201/2011/601842/SER/CLIMA.C2, European Commission, 2012).
15. D. Sherry, A. McCulloch, Q. Liang, S. Reimann, P. A. Newman, Current sources of carbon tertachloride (CCl_4) in our atmosphere. *Environ. Res. Lett.* **13**, 024004 (2018).
16. United Nations, "Montreal Protocol on substances that deplete the ozone layer. Montreal, 16 September 1987. Amendment to the Montreal Protocol on substances that deplete the ozone layer, Kigali, 15 October 2016" (Tech. Rep. C.N.872.2016.TREATIES-XXVII.2.f (Depositary Notification), United Nations, New York, 2016).
17. D. K. Papanastasiou, A. Beltrone, P. Marshall, J. B. Burkholder, Global warming potential estimates for the C_1–C_3 hydrochlorofluorocarbons (HCFCs) included in the Kigali Amendment to the Montreal Protocol. *Atmos. Chem. Phys.* **18**, 6317–6330 (2018).
18. A. Engel, M. Rigby, "Update on ozone-depleting substances (ODSs) and other gases of interest to the Montreal Protocol," in *Scientific Assessment of Ozone Depletion: 2018*, Global Ozone Research and Monitoring Project (Tech. Rep. No. 58, World Meteorological Organization, Geneva, Switzerland, 2018).
19. M. K. Vollmer *et al.*, Abrupt reversal in emissions and atmospheric abundance of HCFC-133a (CF_3CH_2Cl). *Geophys. Res. Lett.* **42**, 8702–8710 (2015).
20. F. Schoenenberger *et al.*, First observations, trends, and emissions of HCFC-31 (CH_2ClF) in the global atmosphere. *Geophys. Res. Lett.* **42**, 7817–7824 (2015).
21. R. Pool, The elusive replacements for CFCs. *Science* **242**, 666–668 (1988).
22. ECETOC, "1,2-Dichloro-1,1-difluoroethane (HFA-133b) CAS:1649-08-7" (Tech. Rep. JAAC 011, European Chemical Industry Ecology and Toxicology Centre, Brussels, Belgium, 1990).
23. ECETOC, "1-Chloro-2,2,2-trifluoroethane (HFA-133a) CAS:75-88-7" (Tech. Rep. JAAC 014, European Chemical Industry Ecology and Toxicology Centre, Brussels, Belgium, 1990).
24. M. W. Anders, Metabolism and toxicity of hydrochlorofluorocarbons: Current knowledge and needs for the future. *Environ. Health Perspect.* **96**, 185–191 (1991).
25. Deutsche Forschungsgemeinschaft, "List of MAK and BAT values 2018: Maximum concentrations and biological tolerance values at the workplace" (Tech. Rep. 54, *Permanent Senate Commission for the Investigation of Health Hazards of Chemical Compounds in the Work Area*, WILEY-VCH Verlag GmbH &Co. KGaA, Weinheim Germany, 2018).
26. J. Burkholder, Ø. Hodnebrog, V. L. Orkin, "Summary of abundances, lifetimes, ozone depletion potentials (ODPs), radiative efficiencies (REs), global warming potentials (GWPs), and global temperature change potentials (GTPs), appendix A" in *Scientific Assessment of Ozone Depletion: 2018*, Global Ozone Research and Monitoring Project (Tech. Rep. No. 58, World Meteorological Organisation, Geneva, Switzerland, 2018).
27. R. G. Prinn *et al.*, History of chemically and radiatively important atmospheric gases from the Advanced Global Atmospheric Gases Experiment (AGAGE). *Earth Syst. Sci. Data* **10**, 985–1018 (2018).
28. S. O'Doherty *et al.*, In situ chloroform measurements at Advanced Global Atmospheric Gases Experiment atmospheric research stations from 1994 to 1998. *J. Geophys. Res.* **10**, 20429–20444 (2001).
29. M. Rigby *et al.*, Recent and future trends in synthetic greenhouse gas radiative forcing. *Geophys. Res. Lett.* **41**, 2623–2630 (2014).
30. S. Henne *et al.*, Validation of the Swiss methane emission inventory by atmospheric observations and inverse modelling. *Atmos. Chem. Phys.* **16**, 3683–3710 (2016).
31. X. Fang *et al.*, Rapid increase of ozone-depleting chloroform emissions from China. *Nat. Geosci.* **12**, 89–93 (2019).

32. M. F. Lunt *et al.*, Continued emissions of the ozone-depleting substance carbon tetrachloride from Eastern Asia. *Geophys. Res. Lett.* **45**, 11423–11430 (2018).
33. Arkema, Proposed closure of the R134a fluorogas activity on the Pierre-Bénite site. https://www.arkema.com/en/media/news/news-details/Proposed-closure-of-the-R134a-fluorogas-activity-on-the-Pierre-Benite-site/, Accessed 12 November 2019 (2016).
34. P. Shanthan Rao, B. Narsaiah, Y. Rambabu, M. Sridhar, V. RK, "Catalytic processes for fluorochemicals: Sustainable alternatives" in *Industrial Catalysis and Separations: Innovations for Process Intensification*, K. V. Raghavan, B. M. Reddy, Eds. (Apple Academic Press, Toronto, Canada, 2015), pp. 407–435.
35. M. K. Vollmer, S. Reimann, M. Hill, D. Brunner, First observations of the fourth generation synthetic halocarbons HFC-1234yf, HFC-1234ze(E), and HCFC-1233zd(E) in the atmosphere. *Environ. Sci. Technol.* **49**, 2703–2708 (2015).
36. R. K. Belter, N. K. Bhamare, Solvent effects in the fluorination of 1,2-dichloro-1,1-difluoroethane (R-132b) to 2-chloro-1,1,1-trifluoroethane (R-133a). *J. Fluor. Chem.* **127**, 1606–1610 (2006).
37. M. K. Vollmer *et al.*, Atmospheric histories and global emissions of the anthropogenic hydrofluorocarbons HFC-365mfc, HFC-245fa, HFC-227ea, and HFC-236fa. *J. Geophys. Res.* **116**, D08304 (2011).
38. P. J. Fraser, R. Langenfelds, N. Derek, L. W. Porter, Studies in air archiving techniques. part 1: Long term stability of atmospheric trace gases in dry, natural air stored in high-pressure, surface-treated aluminum cylinders in *Baseline Atmospheric Program Australia 1989*, S. R. Wilson, J. L. Gras, Eds. (Bureau of Meteorology and CSIRO Division of Atmospheric Research, Canberra, Australia, 1991) Vol. 1989, pp. 16–29.
39. R. L. Langenfelds *et al.*, "The Cape Grim air archive: The first seventeen years, 1978–1995" in *Baseline Atmospheric Program (Australia) 1994-95*, R. J. Francey, A. L. Dick, N. Derek, Eds. (Bureau of Meteorology and CSIRO Division of Atmospheric Research, Australian Bureau of Meteorology and CSIRO Marine and Atmospheric Research, Melbourne, Australia, 1996), pp. 53–70.
40. R. L. Langenfelds *et al.*, "Archiving of Cape Grim air" in *Baseline Atmospheric Program Australia 2009-2010*, N. Derek, P. B. Krummel, S. J. Cleland, Eds. (Australian Bureau of Meteorology and CSIRO Marine and Atmospheric Research, Melbourne, Australia, 2014), pp. 44–45.
41. P. J. Fraser *et al.*, "Non-carbon dioxide greenhouse gases at Cape Grim: A 40 year odyssey" in *Baseline Atmospheric Program (Australia) History and Recollections, 40th Anniversary Special Edition*, N. Derek, P. B. Krummel, S. J. Cleland, Eds. (Bureau of Meteorology and CSIRO Oceans and Atmosphere, Melbourne, Australia, 2016), pp. 45–76.
42. M. K. Vollmer *et al.*, Modern inhalation anesthetics: Potent greenhouse gases in the global atmosphere. *Geophys. Res. Lett.* **42**, 1606–1611 (2015).
43. B. R. Miller *et al.*, Medusa: A sample preconcentration and GC/MS detector system for in situ measurements of atmospheric trace halocarbons, hydrocarbons, and sulfur compounds. *Anal. Chem.* **80**, 1536–1545 (2008).
44. T. Arnold *et al.*, Automated measurement of nitrogen trifluoride in ambient air. *Anal. Chem.* **84**, 4798–4804 (2012).
45. M. Guillevic *et al.*, Dynamic–gravimetric preparation of metrologically traceable primary calibration standards for halogenated greenhouse gases. *Atmos. Meas. Tech.* **11**, 3351–3372 (2018).
46. D. M. Cunnold *et al.*, The atmospheric lifetime experiment 3. Lifetime methodology and application to three years of $CFCl_3$ data. *J. Geophys. Res.* **88**, 8379–8400 (1983).
47. D. M. Cunnold *et al.*, Global trends and annual releases of CCl_3F and CCl_2F_2 estimated from ALE/GAGE and other measurements from July 1978 to June 1991. *J. Geophys. Res.* **99**, 1107–1126 (1994).
48. D. M. Cunnold *et al.*, GAGE/AGAGE measurements indicating reductions in global emissions of CCl_3F and CCl_2F in 1992-1994. *J. Geophys. Res.* **102**, 1259–1269 (1997).
49. M. Rigby *et al.*, Re-evaluation of lifetimes of the major CFCs and CH_3CCl_3 using atmospheric trends. *Atmos. Chem. Phys.* **13**, 2691–2702 (2013).
50. M. K. Vollmer *et al.*, Atmospheric histories and global emissions of halons H-1211 ($CBrClF_2$), H-1301 ($CBrF_3$), and H-2402 ($CBrF_2CBrF_2$). *J. Geophys. Res. Atmos.* **121**, 3663–3686 (2016).
51. J. B. Burkholder *et al.*, "*Chemical kinetics and photochemical data for use in atmospheric studies, evaluation no. 18 of the NASA panel for data evaluation*" (JPL Publication 15-10, Jet Propulsion Laboratory, , Pasadena, CA, 2015).
52. A. F. Ruckstuhl *et al.*, Robust extraction of baseline signal of atmospheric trace species using local regression. *Atmos. Meas. Tech.* **5**, 2613–2624 (2012).
53. A. Stohl, Trajectory statistics—A new method to establish source-receptor relationships of air pollutants and its application to the transport of particulate sulphate in Europe. *Atmos. Environ.* **30**, 579–587 (1996).